

Copper Nanoparticles Stabilized in a Porous Chitosan Aerogel as a Heterogeneous Catalyst for C–S Cross-coupling

Sana Frindy,^[a, b] Abdelkrim el Kadib,^[c] Mohamed Lahcini,^[b] Ana Primo,^{*[a]} and Hermenegildo García^{*[a]}

Cu nanoparticles (NPs) embedded into chitosan fibrils act as a heterogeneous catalyst for the C–S coupling of aryl halides and thiophenol in toluene. The catalyst can be reused under optimal conditions with some activity decrease from the first to the second use. Characterization of the reused catalyst shows that Cu NPs do not undergo agglomeration. Cu-chito-

san is more active for aryl iodides than aryl bromides and chlorides. The presence of chitosan in a large excess is detrimental for the catalytic activity, probably because of the increase of solvent viscosity. It was found that halides formed as byproducts in the reaction act as a catalyst poison and may influence the extent of Cu leaching.

Introduction

Heterogeneous catalysis using metal nanoparticles (MNPs) has become a very important tool to promote many organic reactions.^[1,2] The stabilization of metastable metallic entities against aggregation, with the minimal alteration of the intrinsic catalytic activity, is one of the key points to design highly durable reactive MNPs. Generally, this fundamental prerequisite can be attained by confining MNPs in porous solid supports, wherein the limited available space in the cavities impedes MNP growth and possible interactions with the support may prevent metal leaching from the solid to the liquid phase.^[3,4]

Besides inorganic metal oxides, organic polymers have been used frequently as insoluble MNP supports,^[5,6] and synthetic polymers are used preferentially in comparison to natural biopolymers. However, the last two decades have witnessed an increasing interest in the exploitation of the properties of natural biopolymers in catalysis, particularly with regard to sustainability and environmental issues.^[7,8] Among natural biopolymers, chitosan, a polysaccharide of glucosamine obtained from the partial deacetylation of chitin, meets many required criteria to

be a valuable solid support in the field of catalysis. For instance, although amorphous resins suffer from the burying of catalytic sites within the polymer backbone, which thereby limits the access of reactants, chitosan can be shaped as microspherical beads in which the nanofibrils of the polymer are entangled to form an open 3D network with remarkably high macroporosity and surface area compared to synthetic polymers.^[9] In addition, chitin, from which chitosan is extracted, is the most abundant waste residue in the fishery industry. Chitosan has proven its efficiency for metal ion removal from polluted media and as an insoluble support for transition-metal complexes and active noble MNPs.^[10–15]

The increasing interest for the valorization of biomass wastes as well as the lack of toxicity in these renewable resources prompted us to explore the potential use of chitosan as a support for MNPs. We report the use of chitosan as support of Cu nanoparticles (NPs) and the catalytic activity of the resulting material for the C–S coupling of thiophenol with aryl halides. Coupling reactions catalyzed by transition metals are currently among the most versatile reactions in organic synthesis^[16] and they can be applied not only for cross-coupling C–C reactions but also for the coupling of carbon with heteroatoms, which include O, N, P, and, in particular, S.^[14,17] However, one drawback of the current processes is that many of these coupling reactions are still based on the use of Pd and other noble metals as catalysts. Hence, for economic reasons, there is an urgent need to find an alternative to Pd catalysts based on first-row transition metals.^[18,19] In the present case, the C–S coupling has been performed using Cu as the active metal. If we consider that Cu interacts strongly with amines and N-terminated ligands,^[13] we speculate that the presence of sequential glucosamine units within the chitosan backbone will make this natural biopolymer an adequate support for Cu NPs to form a leaching-resistant catalyst. Precedents in the literature have already shown the use of chitosan as a support of Cu

[a] S. Frindy, Dr. A. Primo, Prof. H. García
Instituto Universitario de Tecnología Química (CSIC-UPV)
Av. de los Naranjos s/n, 46022 Valencia (Spain)
E-mail: aprimoar@itq.upv.es
hgarcia@qim.upv.es

[b] S. Frindy, Prof. M. Lahcini
Laboratory of Organometallic and Macromolecular
Chemistry-Composites Materials
Faculty of Sciences and Technologies
Cadi Ayyad University
Avenue Abdelkrim Elkhattabi, B. P. 549,40000 Marrakech (Morocco)

[c] Prof. A. el Kadib
Euromed Research Institute, Engineering Division
Euro-Mediterranean University of Fes (UEMF), Fès-Shore
Route de Sidi Hrazem, 30070 Fès (Morocco)

Supporting information for this article is available on the WWW under <http://dx.doi.org/10.1002/cctc.201500565>.

complexes or NPs as heterogeneous catalysts for redox and cycloaddition reactions.^[20–23] In a related study, Cu^{II} and Cu^I salts were embedded onto chitosan and used for the coupling of aryl halides and sodium sulfonates to form aryl sulfones.^[24]

Results and Discussion

In the first part of this report, we describe catalyst preparation and provide analytical and spectroscopic evidence for the formation of Cu NPs embedded into the fibrils of chitosan microspheres. In the second part, we describe our investigation of the catalytic activity of these materials for C–S cross-coupling.

Catalyst preparation and characterization

The preparation of Cu-chitosan microspheres was performed in a stepwise manner (Scheme 1). This multistep preparation method consists of the solvothermal formation of Cu NPs starting from Cu(NO₃)₂ dissolved in ethylene glycol and reduction in situ at 150 °C. The solvothermal reduction of Cu²⁺ by heating in ethylene glycol, generally known as the polyol reduction method, is well documented in the literature and is known to render Cu NPs of a small average particle size between 1 and 5 nm.^[25,26] These Cu NPs were supported on chitosan by adding an acidic aqueous solution of this biopolymer to the ethylene glycol solution in which Cu NPs were formed previously, and the mixture was stirred to obtain a homogeneous hydrogel. The formation of highly porous Cu-chitosan microspheres was finally achieved by dropping soluble Cu NPs-chitosan hydrogel into a basic aqueous solution, which causes the instantaneous precipitation of the microspheres. These wet Cu-chitosan microspheres were dried by the gradual replacement of water by ethanol, followed by supercritical CO₂ processing. Previous studies have shown that before supercritical drying, water has to be exchanged completely by ethanol.^[14,27] Otherwise, the direct removal of water affords shrunken xerogels that feature a very low porosity and low surface area because of the operation of strong capillary forces and hydrogen bonding interactions during sudden water removal, which lead to the collapse of porosity in chitosan.^[27]

Three samples were prepared in which the Cu loading was varied from 0.5 to 2.3 wt% by controlling the amount of Cu(NO₃)₂ reduced by ethylene glycol. The above experimental preparation procedure, particularly the supercritical CO₂ drying of alcogels is similar to that used previously for the preparation of chitosan-based solid catalysts.^[13–15,27,28] These reports have shown that supercritical drying allows chitosan particles with

high specific surface area and porosity to be obtained. In the present case, the BET surface area measured by N₂ adsorption isotherm was $\approx 187 \text{ m}^2 \text{ g}^{-1}$, which is significantly lower than the BET surface area of native chitosan, for which a similar drying process allows values around $300 \text{ m}^2 \text{ g}^{-1}$ to be reached. This decrease in the surface area is probably a consequence of the presence of Cu NPs that block some of the pores that would be present in pristine chitosan microspheres.

SEM images of the Cu-chitosan microspheres show the porosity of the bead (Figure 1). Higher magnification shows that

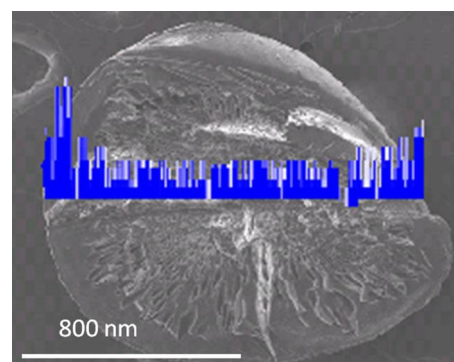
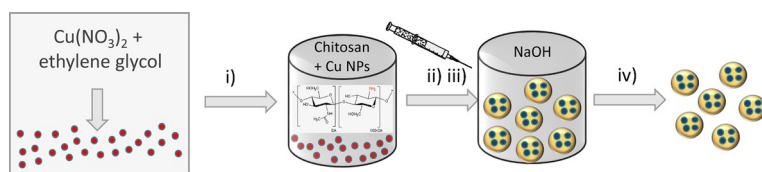


Figure 1. SEM image of Cu-chitosan microspheres that shows the intensity along the bead of the K_α1 line characteristic of Cu in EDX superimposed in blue. The intensity of the K_α1 line is proportional to Cu concentration.

the microspheres are constituted by interwoven fibrils of chitosan polymer that leave an empty space between them. The small size of the Cu NPs prepared by the solvothermal method does not allow the detection of these MNPs at the highest possible magnification used in the SEM study. However, elemental mapping using energy dispersive X-ray (EDX) analysis detects the presence of Cu distributed quasi-homogeneously throughout the microspheres, although there is some higher concentration on the external surface of the bead (Figure 1). In other studies, it was found that MNPs are located preferentially near the external surface, and a gradual decrease of the concentration of the metal is observed on going deeper into the sub-millimeter particle.^[14] In the present case, the fact that the beads have been prepared by the intimate mixing of Cu NPs in dissolved chitosan results apparently in a better dispersion of Cu NPs in the whole polymer bead that are located not only near the external surface but also in similar proportions at the center of the microspheres.

The XRD pattern of Cu-chitosan does not show any peaks characteristic of chitosan because of the amorphous nature of this natural biopolymer. In contrast, despite the low loading of Cu in these materials, its presence is detectable by XRD, and weak peaks at $2\theta = 43.25$, 50.34 , and 74.04° were recorded and assigned unambiguously to the crystalline [111], [200], and [220] facets of metallic Cu NPs (Figure S1). The average particle



Scheme 1. Procedure for the preparation of Cu-chitosan; i) addition of chitosan solution to preformed Cu NPs, ii) addition of chitosan that contains Cu NPs into a NaOH solution, iii) gelification of the chitosan, and iv) supercritical CO₂ drying.

size for the three Cu-chitosan samples under study with Cu loadings of 0.5, 1, and 2.3 wt% could be determined by applying the Scherrer equation using the most intense [111] peak of the diffractogram, and the value was similar for the three samples (≈ 0.5 nm). Thus, no influence of Cu loading on the average particle size at the loading range in this study was observed. Notably, although XRD does not rule out the presence of some Cu atoms in higher oxidation states, it proves the presence of Cu^0 clearly as expected based on previous reports of the solvothermal reduction of Cu in ethylene glycol.^[29–31]

The Cu-chitosan beads were also characterized by high-resolution TEM. This study reveals the presence of homogeneous, ultra-small Cu NPs of 1–2 nm, located throughout the entire bead. Representative TEM images of Cu-chitosan are shown in Figure 2, in which the homogeneous particle size of Cu NPs

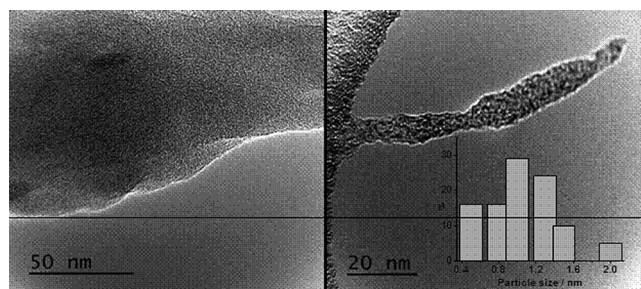


Figure 2. TEM image of a Cu-chitosan microsphere that shows the presence of uniform, small Cu NPs. The inset shows the particle size distribution estimated by counting a statistically relevant number of Cu NPs.

and their distribution in the biopolymer matrix can be observed. A comparison of the Cu NP size distribution of fresh Cu-chitosan and after its use as a catalyst does not show significant changes. This indicates that there is no evident agglomeration of Cu NPs under the reaction conditions. There are precedents in the literature that show that Pd NPs embedded on chitosan also exhibit an average particle size of ≈ 1 nm.^[32] Notably, the average particle size determined by XRD and TEM are within the same range, ≈ 1 nm, which is close to the resolution limit of TEM.

In the case of the Cu-chitosan catalyst, an insightful understanding of the Cu NPs–chitosan interaction in the fresh sample and the changes undergone under the reaction conditions was gained by analysis of the X-ray photoelectron spectra (XPS; Figure 3). For the fresh Cu-chitosan sample, this technique shows the expected C1s, N1s, and O1s peaks, which correspond to chitosan, together with a Cu2p peak. The XPS C1s peak can be deconvoluted into three components of a relative proportion of 23, 30, and 6%, the positions of which are attributed to C bonded to C (binding energy (BE) = 284.5 eV), C bonded to N (BE = 286.7 eV), and C bonded to O (BE = 288.5 eV). Furthermore, the spectrum of the fresh catalyst shows the N1s peak at BE = 400.0 eV. This shift to a higher binding energy (compared to BE = 399 eV for NH_2 in native chitosan) suggests a dative coordination of NH_2 to Cu NPs ($\text{NH}_2 \rightarrow \text{Cu}$). A similar shift for the N1s BE has been observed for a set of chitosan-metal oxide hybrid materials for which the dona-

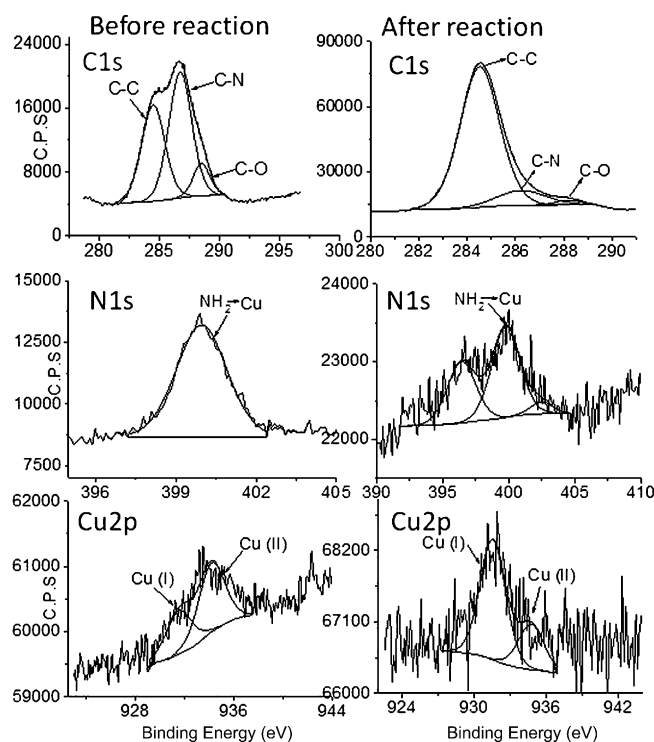


Figure 3. XPS peaks that correspond to Cu-chitosan and the best deconvolution to individual components. Left: fresh Cu-chitosan; right: Cu-chitosan after four consecutive uses as a catalyst in the C–S cross-coupling of thiophenol and iodobenzene.

tion of the N atom to the metal centers ($\text{NH}_2 \rightarrow \text{M}$, $\text{M} = \text{Ti}, \text{Zr}, \text{Al}, \text{V}, \text{W}, \text{Mo}$) has been proposed.^[15,33,34] The spectrum of the fresh Cu-chitosan catalyst shows a weak Cu2p peak that can be deconvoluted into two individual components with maxima at BE = 931.5 (0.07%) and 934.3 eV (0.1%) that correspond to the contributions of Cu^{I} and Cu^{II} , respectively. The assignment of Cu^{I} was confirmed by observation of the corresponding Auger peak with a kinetic energy of 916.5 eV. Notably, there is an apparent discrepancy between the detection of Cu^{I} and Cu^{II} by XPS and Cu^0 NPs by XRD and TEM. This discrepancy has been observed frequently in metals and is because XPS is a surface technique that only reports on the shallow thin layer of the material of a few nm, whereas the other techniques report on the bulk of the material. Thus, most probably exposure to the air has formed a thin layer of Cu oxides on the external surface of Cu-chitosan. For this reason and to ensure the reproducibility of the catalytic results, Cu-chitosan materials were submitted to a preactivation step immediately before their use as catalyst that consists of reduction with H_2 at 200 °C.

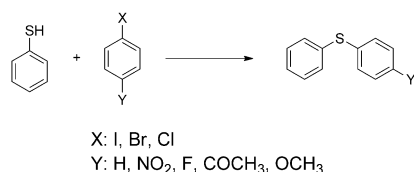
After four consecutive uses as a catalyst for the C–S coupling of thiophenol and iodobenzene, significant changes were observed by XPS both in Cu NPs and the chitosan support. The most remarkable changes are related to the significant decrease in the percentage of external N atoms, the atomic proportion of which decreases from 5 to 0.1%, and at the same time the XPS peak splits and exhibits a new component at a significantly lower BE of 396.4 eV, which corresponds to N atoms not coordinated to Cu. This decrease in the N con-

ment is also reflected in the C 1s peak, which becomes simpler, and the contribution of C atoms bonded to N observed previously is almost absent. Besides the change in chitosan, the XPS Cu2p peak also undergoes remarkable changes (Figure 3). Although the total concentration of Cu atoms at the surface does not vary and remains constant, the contribution of the Cu^{II} component at BE=934.76 eV almost disappears and only the peak for Cu^I at BE=931.5 eV remains. This change could be the result of the activation of the catalyst by H₂ at 200 °C before the reaction and/or to the reduction by I⁻ ions formed during the reaction that leads to some I₂ and Cu^I. In any case, XPS evidences clearly that as consequence of the reaction, the external surface of chitosan loses N atoms and that the active sites of the reaction seem to be Cu in low oxidation states, probably Cu⁰ and Cu^I.

Further insight on the interplay between the Cu NPs and chitosan support has been gained by FTIR spectroscopy. Indeed, besides the typical signals of the carbohydrate scaffold recognized in Cu-chitosan, the band assigned to -NH₂ disappeared, and we observed a new shoulder at $\tilde{\nu}=1557\text{ cm}^{-1}$, which indicates a weak interaction of the NH₂ fragment with Cu NPs. This shift to lower values is typical for hybrid materials that exhibit an interaction between chitosan and its metal or metal oxide partner. As an illustration, a shift to $\tilde{\nu}=1520\text{ cm}^{-1}$ has been observed for chitosan-vanadium oxide^[15] and for chitosan-stabilized Au NPs,^[14] in which NH₂→V and NH₂→Au take place, respectively. Similar values were also observed for chitosan-sepiolite^[35] and chitosan-montmorillonite hybrid materials.^[36]

Catalytic study

Three samples of Cu-chitosan that have Cu loadings of 0.5, 1, and 2.3 wt%, determined by inductively coupled plasma optical emission spectroscopy (ICP-OES), were evaluated as catalysts for the coupling of thiophenol and iodobenzene to form diphenyl sulfide in toluene as the solvent at 130 °C (Scheme 2). The time-conversion plots for these three catalysts are shown



Scheme 2. C-S coupling of thiophenol and aryl halides to form diaryl sulfides.

in Figure 4. The initial reaction rate and performance of the catalyst increase with the Cu loading; the best-performing Cu-chitosan sample is the one with the highest Cu loading. This pattern contrasts with the typical trend observed commonly for supported MNPs in which the catalytic activity generally increases as the loading of metal on the support decreases if the metal/substrate molar ratio is maintained because of the smaller particle size and higher metal dispersion that can be achieved

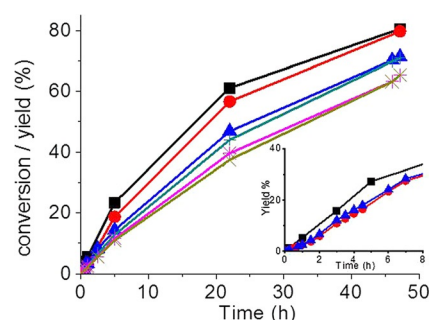


Figure 4. Time-conversion plots for the C-S coupling of thiophenol and iodobenzene catalyzed by Cu-chitosan as a function of the Cu loading on chitosan. ■ conversion and ● yield for Cu-chitosan with 2.3 wt% of Cu; ▲ conversion and + yield for Cu-chitosan with 1 wt% of Cu; * conversion and × yield for Cu-chitosan with 0.5 wt% of Cu. Inset: ■ diphenyl sulfide yield from 2 mol% Cu-chitosan as catalyst; ● yield of diphenyl sulfide using 2 mol% Cu-chitosan with 50 wt% chitosan; ▲ yield of diphenyl sulfide in the presence of 2 mol% Cu-chitosan with 100 wt% chitosan. Reaction conditions: 1 mmol of iodobenzene, 1.2 mmol of thiophenol, 3 mL of toluene, 130 °C, 3 mmol of NEt₃, 2 mol% of catalyst.

for low loadings. In this case, it could be that the amount of chitosan plays a negative role in the catalytic reaction. To maintain the Cu/substrate molar ratio while we vary the Cu loading on the support, the amount of chitosan support has to be over four times higher at 0.5 wt% loading than that at 2.3 wt% in Cu-chitosan.

After we selected the most convenient Cu NP loading on chitosan as 2.3 wt%, additional experiments to optimize the Cu/substrate mol ratio were performed (Figure 5). Indeed, the

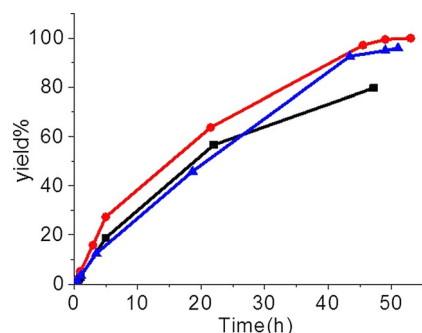


Figure 5. Time-yield plots for the reaction of thiophenol and iodobenzene catalyzed by Cu-chitosan as a function of Cu loading on the support ● 2 mol%; ▲ 4 mol%; ■ 1 mol%. Reaction conditions: 1 mmol of iodobenzene, 1.2 mmol of thiophenol, 3 mL of toluene, 130 °C, 3 mmol of NEt₃.

initial reaction rates at Cu/substrate molar ratios of 1 and 4% are identical, and the optimal Cu/substrate molar ratio is 2%. Again, this effect of the increase of Cu/substrate molar ratio unusual as it is expected that the reaction rate should increase along with the Cu/substrate molar ratio. The fact that there is an optimal ratio of 2 mol% could be the consequence of two opposite effects. On one hand, the reaction rate should increase with the amount of Cu present, but on the other hand the presence of higher amounts of chitosan should be detrimental as stated previously. Therefore, a balance between these two opposite effects leads to a compromise, and the

highest performance is reached at a Cu/substrate molar ratio of 2%.

To provide experimental evidence in support of the negative role that an excess of chitosan can play on the catalytic activity of the Cu NPs for the C–S coupling, a series of experiments using Cu-chitosan as the catalyst to which additional amounts of unmodified chitosan was added were performed. The results are presented inset in Figure 4. As illustrated above, Cu-chitosan in the absence of any added chitosan exhibits the highest initial reaction rate and diphenyl sulfide yield at the final time.

The addition of 50 or 100 wt% of chitosan decreases both the initial reaction rate and the diphenyl sulfide yield. This negative effect of chitosan addition increases, although not linearly, if the amount of chitosan added was doubled. Therefore, it can be concluded that although the presence of chitosan as the support is necessary to confine and stabilize the Cu NPs to allow their recovery and separation from the reaction mixture, an increase in the amount in chitosan to values higher than the minimum necessary plays an undesirable role by decreasing the activity of the Cu catalyst. One possible way in which chitosan can have a negative effect on the reaction is by increasing the viscosity of the reaction medium or by adsorbing reagents and (by)products, which blocks the Cu active sites.

After the optimization of Cu loading on chitosan and the Cu/substrate molar ratio, the influence of solvent on the reaction was studied. Notably, the variation of the nature of the solvent is accompanied unavoidably by the variation of the base used in the reaction because of solubility limitations. Specifically, the coupling of thiophenol and iodobenzene with KOH in acetonitrile, Na_2PO_4 in 1,4-dioxane, and NEt_3 in toluene were screened. The temporal profile of the C–S coupling reaction in each of these solvent/base pairs is shown in Figure 6. Indeed, the lowest reaction rate was observed for 1,4-dioxane, and the fastest transformation took place in acetonitrile. Unfortunately, chemical analysis of the liquid phase after the removal of the solid catalyst showed that the acetonitrile contained a significant amount of the total Cu present initially in the catalyst, which indicates the occurrence of a high degree of Cu leaching. The occurrence of leaching is favored by relatively long reaction times and high temperatures. In contrast,

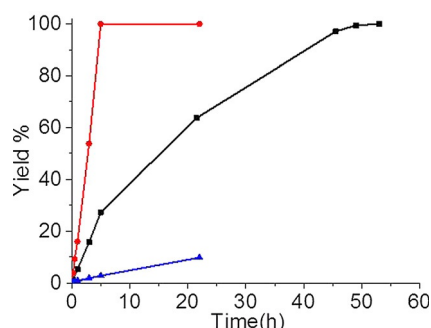


Figure 6. Time–yield plot for the reaction of thiophenol and iodobenzene catalyzed by Cu-chitosan in three combinations of solvent and base: ● acetonitrile/KOH; ■ toluene/ Et_3N ; ▲ 1,4-dioxane/ Na_2PO_4 . Reaction conditions: 1 mmol of iodobenzene, 1.2 mmol of thiophenol, 3 mL of solvent, 130 °C, 3 mmol of base, 2 mol% of catalyst.

Cu leaching in toluene as a solvent and NEt_3 as base was significantly lower (2% of the initial Cu content of the catalyst, 25 μg in 3 mL) and at the same time exhibits an adequate initial reaction rate. It could be that compared to Pd, Cu is more prone to undergo leaching and becomes partly dissolved in organic solvents. There are precedents in the literature that show the absence of metal leaching in the case of Pd NPs embedded in chitosan in xylene at 130 °C for ≈ 7 h.^[37] Accordingly, toluene was selected for subsequent studies on the catalytic activity of Cu-chitosan.

The next parameter that was optimized was the reaction temperature. As a result of its structure, there is a limitation of the maximum temperature that chitosan can stand without becoming dissolved or undergoing a substantial change of the morphology of its particles.^[38] In the present case, the influence of the temperature on the catalytic activity of Cu-chitosan was determined in the range of 120–150 °C, and the results are presented in Figure 7. The initial reaction rate increases with

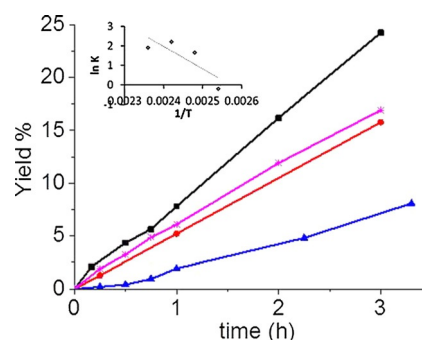
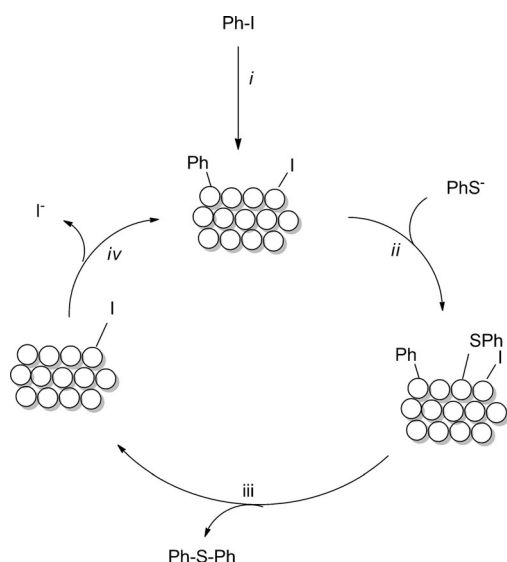


Figure 7. Influence of the temperature on the time–yield plot for the reaction of thiophenol and iodobenzene catalyzed by Cu-chitosan ■ 140, ● 130, ▲ 120, * 150 °C; Reaction conditions: 1 mmol of iodobenzene, 1.2 mmol of thiophenol, 3 mL of toluene, 3 mmol of NEt_3 , 2 mol% of catalyst. Inset: Arrhenius plot of the logarithm of the initial reaction rate versus the reciprocal of the absolute temperature.

the temperature from 120 to 140 °C but then diminishes at 150 °C. This lower initial reaction rate observed at 150 °C is related to variations of the morphology of chitosan spheres at this temperature and, accordingly, it represents the temperature limit in this case. The influence of temperature on the initial reaction rate in the range of 120–140 °C allows us to determine the activation energy of the process ($E_a = 95.5 \text{ kJ mol}^{-1}$) from the Arrhenius plot (Figure 7, inset). In view of the above data, 130 °C was selected as a convenient temperature to perform C–S couplings using Cu-chitosan as the catalyst.

According to the previous characterization data that show the presence of low-oxidation Cu^0 and Cu^I states, the most reasonable reaction mechanism for the C–S coupling compatible with the literature^[39] is proposed in Scheme 3. We propose that Ph–I splits on the Cu NP surface to form Cu–Ph and Cu–I species. Similarly, in the presence of base, Ph–S[−] anions should also bind to the Cu NP surface. Thus, the surface of Cu NP should have a population of adsorbed phenyl, phenylthio, and iodo species on different sites. C–S coupling will take place on



Scheme 3. Simplified mechanistic proposal for C–S coupling on Cu NPs.
i) Ph–I splitting on low-coordinate Cu atoms on the surface; ii) Adsorption of PhS^- on the surface; iii) PhSPh desorption; iv) I^- desorption.

the Cu NP surface, and the subsequent desorption of Ph–SPh and I^- will complete the catalytic cycle.

An important issue in heterogeneous catalysis is to show the stability of the catalyst under the reaction conditions. To test the reusability of Cu-chitosan in toluene, a series of consecutive reactions between iodobenzene and thiophenol were performed using the same catalyst sample. At the end of each reaction, the solid catalyst was recovered by filtration, washed with fresh toluene, and used in a consecutive reaction under the same conditions. The temporal profile of diphenyl sulfide formation in consecutive runs is presented in Figure 8. Although the initial reaction rate of the fresh catalyst was significantly higher than that in the subsequent reuses, the differences in the initial reaction rate and yield at the final time from the second to the fifth reuses were relatively minor. To understand this pattern, chemical analysis of the Cu present in the liquid phase in each of the consecutive runs was performed. As noted earlier, the chemical analysis of toluene in the first run revealed the presence of a small amount of Cu (2.3% of

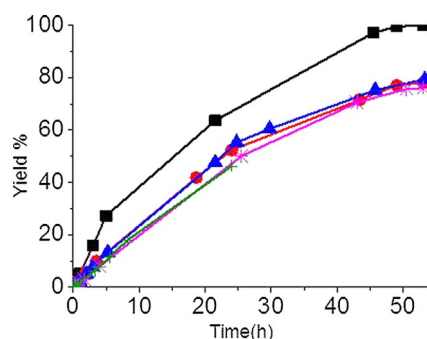


Figure 8. Time–yield plot for the reuse of Cu-chitosan; ■ run 1, ● run 2, ▲ run 3, * run 4; + run 5. Reaction conditions: 1 mmol of iodobenzene, 1.2 mmol of thiophenol, 3 mL of toluene, 130 °C, 3 mmol of NEt_3 , 2 mol% of Cu catalyst.

the initial Cu amount present in the catalyst). The extent of Cu leaching was almost the same in the subsequent reactions (2.23 and 2.17 wt%). Based on these analytical data, it appears that the leaching of Cu into toluene is not responsible for the change from the fresh to the used catalyst and it is more likely that changes in the porosity and structure of the chitosan beads should be responsible for this decrease in activity upon reuse. It is proposed that a reorganization of the porosity takes place in the first run and, then, the resultant Cu-chitosan is considerably more stable from a catalytic point of view and maintains its structure relatively unaltered in subsequent runs. Below, we will comment on other deactivation pathways that also occur as consequence of the formation of iodide as by-product during the course of the reaction.

One general feature in cross-coupling reactions is the much higher reactivity of iodides with respect to bromides, and aryl chlorides are notoriously less reactive. This general trend is a consequence of the C–X bond strength and its influence on the kinetics of the reaction in which the rate-determining step involves the cleavage of this bond. As expected, Cu-chitosan was inactive to promote the C–S coupling of thiophenol with bromo- or chlorobenzene. However, if a nitro group, which activates the C–X bond, is present, then C–S coupling between 2- and 4-nitrobromobenzene and 4-nitrochlorobenzene takes place. The initial reaction rate and final conversion depend on the substrate and follow the order 4-nitrochlorobenzene < 4-nitrobromobenzene \approx 2-nitrobromobenzene < iodobenzene (Figure 9). Although the initial reaction rate should be a function of the nature and strength of the C–X bond, it was observed that the final yield also follows the order of the initial rate.

The conversion of both 4-nitrobromobenzene and 4-nitrochlorobenzene stops after ≈ 25 h (Figure 9). This could indicate catalyst deactivation. To verify this possibility and to understand the origin of the possible deactivation, the reaction of thiophenol and iodobenzene was selected as a model and 0.1 equivalents of NaX (X: I^- , Br^- , and Cl^-) was added on purpose as a possible poison. As the C–S coupling progresses, an increasing build-up of the X^- concentration should develop as byproduct of the coupling, and it was reasoned that this halide could act as a poison to deactivate the catalyst because

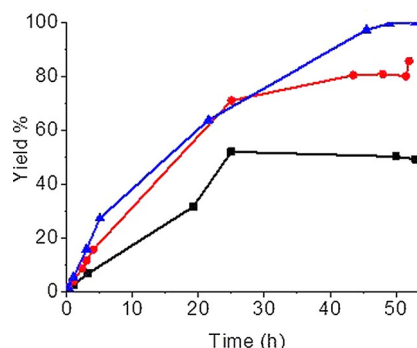


Figure 9. Time–yield plots for the coupling of thiophenol with substituted aryl halides. ▲ iodobenzene; ● 4-nitrobromobenzene; ■ 4-nitrochlorobenzene. Reaction conditions: 1 mmol of aryl halide, 1.2 mmol of thiophenol, 3 mL of toluene, 130 °C, 3 mmol of NEt_3 , 2 mol% of catalyst.

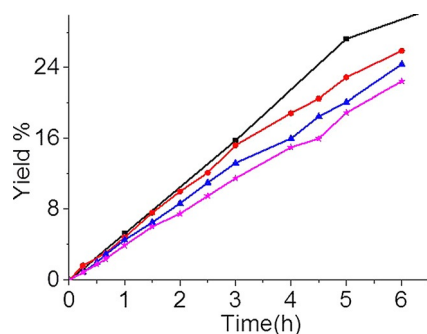


Figure 10. Influence of the absence or presence of NaX on the time–yield plot for the reaction of thiophenol and iodobenzene catalyzed by Cu-chitosan: ■ without base; ● NaI; ▲ NaBr; * NaCl. Reaction conditions: 1 mmol of iodobenzene, 1.2 mmol of thiophenol, 3 mL of toluene, 130 °C, 3 mmol of NEt_3 , 2 mol% of catalyst.

of a strong Cu–X interaction. The results of the influence of NaX on the catalytic activity of Cu-chitosan are shown in Figure 10. The initial reaction rate and product yield at 6 h decrease gradually in the order of $\text{X}^- > \text{I}^- > \text{Br}^- > \text{Cl}^-$. These kinetic data support the role of the halide as a catalyst poison, and the poisoning effect increases with the strength of the Cu–X interaction.

According to these data, aryl chlorides as substrates are not only the least reactive because of the strength of the C–Cl bond but also the chloride formed as a byproduct displays a strong inhibitory effect attributed to its strong Cu–Cl bond compared to the other acyl halides. This poisoning effect is responsible for the deactivation of the catalyst as the reaction progresses, which stops the reaction before it reaches the equilibrium concentration.

Another possible effect of the interaction of halides with Cu NPs is to increase the Cu leaching from the solid to the solution. In MNPs and particularly in catalysis by supported Au NPs in which HAuCl_4 is the most frequent precursor, it has been found that the presence of residual amounts of Cl^- from the precursor is highly detrimental from the point of view of the stability of the catalyst.^[40,41] The presence of Cl^- on the Au catalyst increases the Au NPs particle size, an effect that has been attributed to the ability of Cl^- to mobilize metal atoms.^[42] We were also interested to determine if besides deactivation, the presence of Cl^- as a mobilizing agent increases Cu leaching from the Cu-chitosan solid to toluene. To check this possibility, a series of experiments in which Cu-chitosan was heated at the reaction temperature in toluene that contained increasing amounts of $(\text{Bu})_4\text{NCl}$ was performed. This quaternary ammonium chloride was selected to overcome the solubility problems of NaCl and other inorganic chlorides in toluene. After 6 h reaction, the solid catalyst was removed by filtration, and the clear toluene solution was analyzed for its Cu content. The results are presented in Table 1 and they show clearly that although no Cu was detected in the liquid phase in the absence of Cl^- , the Cu content in toluene increases as the concentration of Cl^- increases. Accordingly, it can also be expected that one of the main reasons for Cu leaching in the present C–S coupling reaction could be the complexation of Cu with X^-

Cl^- conc. [ppm]	Initial Cu amount [mg]	Cu amount leached [μg]	Proportion of initial Cu leached to toluene [%]
0	0.7	0	0
0.25	0.7	1.1	0.15
1.25	0.7	3.4	0.48

that can facilitate the dissolution and leaching of Cu. This effect should be especially important in the case of Cl^- for which the interactions with Cu are stronger.

To gain a deeper insight into the possible changes that occur in Cu-chitosan during catalysis, the solid catalyst was recovered after the fourth run and characterized by TEM and XRD. Selected TEM images of the Cu-chitosan used four times and EDX analysis of Cu-chitosan after this consecutive reuse as a catalyst are presented in Figure 11. As in the case of the fresh Cu-chitosan material, EDX elemental mapping of the microsphere indicates that Cu is still present homogeneously and highly dispersed in the form of nanometric particles through-

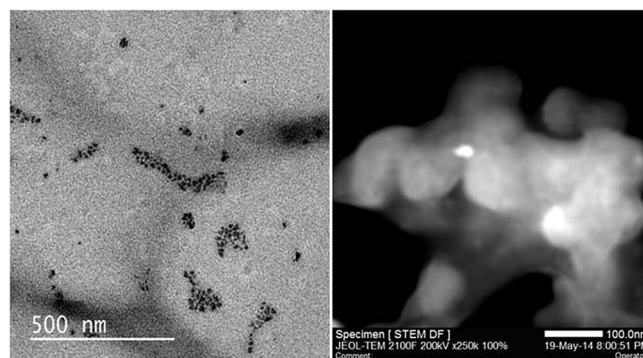


Figure 11. TEM and bright-field SEM images of four times reused Cu-chitosan. The images show that Cu is distributed all over the chitosan beads.

out the beads. In XRD, fresh Cu-chitosan shows the pattern that corresponds to metallic Cu, although the peaks are weak (Figure S1). In contrast, after reuse this diffraction peak is barely detectable or disappears (Figure S1). This could indicate either a decrease on the average Cu NP size or the occurrence of Cu leaching with a decrease of the total Cu loading. The second possibility seems less likely if we consider that chemical analysis of the solution showed that the accumulated amount of Cu leaching in the fourth reuse was below 10% of the initial Cu content (127 μg leached Cu out from 1.27 mg Cu-chitosan). In any case, it can be concluded that the Cu NPs do not agglomerate during the catalytic reaction.

Finally, the scope of the reaction was screened beyond the parent Ph_2S and nitro derivative by performing a series of C–S couplings using Cu-chitosan as the catalyst, and the results are shown in Table 2. The C–S coupling promoted by Cu-chitosan seems to be general for aryl iodides, although the yield depends on the substituent, and electron-withdrawing substitu-

Table 2. Results of the C–S coupling catalyzed by Cu-chitosan. Reaction conditions: 0.5 mmol of iodobenzene, 0.6 mmol of thiophenol, 3 mL of toluene, 130 °C, 3 mmol of NEt₃, 2 mol % of catalyst.

Entry	Substrate X- <i>p</i> -C ₆ H ₄ -Y	C–S coupling product yield [%]
1	X = I; Y = H	96; ^[a] 92 ^[b]
2	X = Br; Y = H	0
3	X = I; Y = NO ₂	99; ^[a] 88 ^[b]
4	X = Br; Y = NO ₂	84; ^[a] 77 ^[b]
5	X = Cl; Y = NO ₂	46; ^[a] 40 ^[b] (isolated 38)
6	X = I; Y = F	86 ^[b]
7	X = I; Y = COCH ₃	87 ^[b]
8	X = I; Y = OCH ₃	44 ^[b]

[a] Determined by GC using dodecane as internal standard; [b] Determined by ¹H NMR spectroscopy of the reaction mixture using *p*-dimethoxybenzene as internal standard.

ents afford higher yields. Unactivated phenyl bromide fails to give the C–S coupling product. In contrast, nitro-substituted aryl halides render the *p*-nitro diphenyl sulfide in various yields, which depends on the halide, as commented on earlier.

Conclusions

We have shown that highly dispersed Cu nanoparticles (NPs) can be prepared and embedded within the chitosan fibril matrix. The resulting microspheres exhibit catalytic activity for C–S coupling. The presence of a large amount of chitosan is detrimental for the catalytic activity, probably because of solution viscosity changes or reagent adsorption and, accordingly, there is an optimal value for the Cu loading on chitosan and the Cu/substrate molar ratio. The catalyst can be reused under optimal conditions at least four times, but a decrease in the activity from the first to the second use is noticed accompanied by minor Cu leaching. Cu-chitosan is more active for aryl iodides than aryl bromides and chlorides. Catalytic tests have shown that halides released during the reaction may act as a poison for Cu NPs and as mobilizers of Cu atoms, which increase the leaching of Cu to the solution, particularly Cl⁻. The characterization of the catalyst after use reveals the absence of Cu NP agglomeration, but a decrease in the average particle size is observed based on the disappearance of the characteristic Cu peaks in the XRD pattern. If we consider the wide availability of chitosan, which can be obtained in large amounts as waste of the fishery industry, and that Cu is a widely abundant transition metal, Cu-chitosan has many advantages from a sustainability point of view and exhibits an adequate activity for the C–S coupling with aryl iodides.

Experimental Section

General remarks

Commercially available reagents and solvents were purchased from Across and Aldrich and used without further purification. Chitosan of medium molecular weight and a deacetylation degree of 80% was purchased from Sigma-Aldrich. All the C–S coupling products have been reported in the literature and were character-

ized by GC–MS and ¹H and ¹³C NMR spectroscopy of the reaction mixtures.

Characterization

SEM images were acquired by using a JEOL JSM 6300 apparatus. TEM images were recorded by using a Philips CM 300 FEG system with an operating voltage of 100 kV. Diffuse reflectance infrared Fourier transform spectroscopy (DRIFTS) was performed by using a NICOLET iS10 spectrometer. XPS were recorded by using a SPECS spectrometer equipped with a Phoibos 150 9MCD detector using a non-monochromatic X-ray source (Al and Mg) operating at 200 W. The samples were evacuated in the prechamber of the spectrometer at 1 × 10⁻⁹ mbar. Some of the samples were activated in situ by N₂ flow at 450 °C for 3 h, followed by evacuation at 10⁻⁸ mbar. The measured intensity ratios of the components were obtained from the area of the corresponding peaks after nonlinear Shirley-type background subtraction and corrected by the transmission function of the spectrometer. Quantitative ICP-OES measurements were performed by using a 715-ES Varian apparatus. BET analysis was performed by using a Micromeritics ASAP2420 instrument. GC was performed by using a Bruker 430-GC instrument equipped with a flame-ionization detector (FID) and a HP-5MS column (30 m × 0.25 mm × 0.25 mm), the stationary phase of which is constituted by cross-linked 5% phenylmethylsilicone, using *n*-dodecane as standard. A known weight of *n*-dodecane was added to an aliquot of the reaction diluted in CH₂Cl₂, and the resulting solution (10 mL) was injected into the GC (250 °C injector temperature). The product yields were determined by ¹H NMR spectroscopy of the reaction mixture after the addition of *p*-dimethoxybenzene as the internal standard by using a 300 MHz Varian Gemini Instrument and CDCl₃ as the solvent.

Catalyst preparation

Preparation of Cu NPs

Cu NPs were synthesized by solvothermal reduction in ethylene glycol. Briefly, Cu(NO₃)₂ (0.054 g) was dissolved in ethylene glycol (0.5 mL). The mixed solution was heated for 24 h at 150 °C under reflux. After the solution was cooled, a chitosan solution (0.5 g of chitosan in 28 mL of 1% v/v acetic acid solution) was added dropwise, and the mixture was stirred until the total dispersion of Cu. Then, this solution was added dropwise into a NaOH solution (4 M) by using a syringe with a 0.8 mm needle. The Cu-chitosan microspheres were aged in the alkaline solution for 24 h and then filtered and washed until a neutral pH solution was obtained. The hydrogel microspheres were first dehydrated by immersion for 30 min with stirring in a series of successive ethanol/water baths of increasing alcohol concentration (10, 30, 50, 70, 90, and 100 v/v%). Finally, Cu-chitosan aerogel microspheres were formed by supercritical CO₂ drying (73.8 bar, 31.5 °C) by using a Polaron 3100 apparatus.

C–S coupling reaction

Typically, iodobenzene (1 mmol), thiophenol (1.2 mmol), and Et₃N (3 mmol) were dissolved in toluene (3 mL). Then, the catalyst (2 mol % of Cu respect to iodobenzene) was added. The reaction mixture pressurized with Ar (5 bar) was stirred and placed in a preheated silicon bath and heated at 130 °C for 60 h. The reaction progress was monitored by periodic analysis of aliquots of the liquid phase by GC using *n*-dodecane as the external standard.

Reusability of heterogeneous Cu-chitosan catalysts

After the completion of the first cycle as described above, the Cu-chitosan microspheres were recovered from the reaction mixture by filtration and washed with toluene three times. The recycled Cu-chitosan catalyst was used again in the next coupling reaction under the same reaction conditions.

Acknowledgements

Financial support by the Spanish Ministry of Economy and Competitiveness (Severo Ochoa and CTQ-2012-32315) is gratefully acknowledged. S.F. thanks the EMAG for a fellowship to support her stage at Valencia.

Keywords: copper · cross-coupling · heterogeneous catalysis · nanoparticles · polymers

- [1] A. Corma, H. García, *Chem. Soc. Rev.* **2008**, *37*, 2096–2126.
- [2] D. Astruc, F. Lu, J. Ruiz Aranzaes, *Angew. Chem. Int. Ed.* **2005**, *44*, 7852–7872; *Angew. Chem.* **2005**, *117*, 8062–8083.
- [3] A. Roucoux, J. Schulz, H. Patin, *Chem. Rev.* **2002**, *102*, 3757–3778.
- [4] Y. Wang, Z. Xiao, L. Wu, *Curr. Org. Chem.* **2013**, *17*, 1325–1333.
- [5] M. Králik, A. Biffis, *J. Mol. Catal. A* **2001**, *177*, 113–138.
- [6] J. Lu, P. H. Toy, *Chem. Rev.* **2009**, *109*, 815–838.
- [7] L. F. Xiao, F. W. Li, C. G. Xia, *Appl. Catal. A* **2005**, *279*, 125–129.
- [8] A. Kadib, M. Bousmina, D. Brunel, *J. Nanosci. Nanotechnol.* **2014**, *14*, 308–331.
- [9] A. El Kadib, M. Bousmina, *Chem. Eur. J.* **2012**, *18*, 8264–8277.
- [10] M. G. Dekamin, M. Azimoshan, L. Ramezani, *Green Chem.* **2013**, *15*, 811–820.
- [11] P. K. Sahu, P. K. Sahu, S. K. Gupta, D. D. Agarwal, *Ind. Eng. Chem. Res.* **2014**, *53*, 2085–2091.
- [12] D. A. Barskiy, K. V. Kovtunov, A. Primo, A. Corma, R. Kaptein, I. V. Kopytyug, *ChemCatChem* **2012**, *4*, 2031–2035.
- [13] M. Chtchigrovsky, A. Primo, P. Gonzalez, K. Molvinger, M. Robitzer, F. Quignard, F. Taran, *Angew. Chem. Int. Ed.* **2009**, *48*, 5916–5920; *Angew. Chem.* **2009**, *121*, 6030–6034.
- [14] A. Primo, F. Quignard, *Chem. Commun.* **2010**, *46*, 5593–5595.
- [15] A. El Kadib, A. Primo, K. Molvinger, M. Bousmina, D. Brunel, *Chem. Eur. J.* **2011**, *17*, 7940–7946.
- [16] G. Dyker, *Angew. Chem. Int. Ed.* **1999**, *38*, 1698–1712; *Angew. Chem.* **1999**, *111*, 1808–1822.
- [17] G. Y. Li, *Angew. Chem. Int. Ed.* **2001**, *40*, 1513–1516; *Angew. Chem.* **2001**, *113*, 1561–1564.
- [18] N. Miyaura, A. Suzuki, *Chem. Rev.* **1995**, *95*, 2457–2483.
- [19] F. S. Han, *Chem. Soc. Rev.* **2013**, *42*, 5270–5298.
- [20] R. B. N. Baig, R. S. Varma, *Green Chem.* **2013**, *15*, 1839–1843.
- [21] Y. Chang, Y. Wang, F. Zha, R. Wang, *Polym. Adv. Technol.* **2004**, *15*, 284–286.
- [22] E. Guibal, *Prog. Polym. Sci.* **2005**, *30*, 71–109.
- [23] A. V. Kucherov, N. V. Kramareva, E. D. Finashina, A. E. Koklin, L. M. Kustov, *J. Mol. Catal. A* **2003**, *198*, 377–389.
- [24] C. Shen, J. Xu, W. Yu, P. Zhang, *Green Chem.* **2014**, *16*, 3007–3012.
- [25] K. J. Carroll, J. U. Reveles, M. D. Shultz, S. N. Khanna, E. E. Carpenter, *J. Phys. Chem. C* **2011**, *115*, 2656–2664.
- [26] B. K. Park, S. Jeong, D. Kim, J. Moon, S. Lim, J. S. Kim, *J. Colloid Interface Sci.* **2007**, *311*, 417–424.
- [27] R. Valentin, K. Molvinger, F. Quignard, D. Brunel, *New J. Chem.* **2003**, *27*, 1690–1692.
- [28] A. Primo, M. Liebel, F. Quignard, *Chem. Mater.* **2009**, *21*, 621–627.
- [29] C.-Y. Lu, M.-Y. Wey, Y.-H. Fu, *Appl. Catal. A* **2008**, *344*, 36–44.
- [30] W. Yu, H. Xie, L. Chen, Y. Li, C. Zhang, *J. Dispersion Sci. Technol.* **2010**, *31*, 364–367.
- [31] H. Kawasaki, R. Arakawa, 32 pp., Chemical Indexing Equivalent to 161:758379 (JP), **2013**.
- [32] M. Adlim, M. Abu Bakar, K. Y. Liew, J. Ismail, *J. Mol. Catal. A* **2004**, *212*, 141–149.
- [33] A. El Kadib, K. Molvinger, M. Bousmina, D. Brunel, *J. Catal.* **2010**, *273*, 147–155.
- [34] A. Aqil, A. El Kadib, M. Aqil, M. Bousmina, A. Elidrissi, C. Detrembleur, C. Jérôme, *RSC Adv.* **2014**, *4*, 33160–33163.
- [35] M. Darder, M. López-Blanco, P. Aranda, A. J. Aznar, J. Bravo, E. Ruiz-Hitzky, *Chem. Mater.* **2006**, *18*, 1602–1610.
- [36] A. El Kadib, K. Molvinger, T. Cacciaguerra, M. Bousmina, D. Brunel, *Microporous Mesoporous Mater.* **2011**, *142*, 301–307.
- [37] B. C. E. Makhubela, A. Jardine, G. S. Smith, *Appl. Catal. A* **2011**, *393*, 231–241.
- [38] A. El Kadib, *ChemSusChem* **2015**, *8*, 217–244.
- [39] S. V. Ley, A. W. Thomas, *Angew. Chem. Int. Ed.* **2003**, *42*, 5400–5449; *Angew. Chem.* **2003**, *115*, 5558–5607.
- [40] A. S. K. Hashmi, G. J. Hutchings, *Angew. Chem. Int. Ed.* **2006**, *45*, 7896–7936; *Angew. Chem.* **2006**, *118*, 8064–8105.
- [41] G. J. Hutchings, *Catal. Today* **2005**, *100*, 55–61.
- [42] B. Nkosi, N. J. Coville, G. J. Hutchings, M. D. Adams, J. Friedl, F. E. Wagner, *J. Catal.* **1991**, *128*, 366–377.

Received: May 20, 2015

Published online on September 1, 2015